Morphological investigation at the front and rear surfaces of fused silica processed with femtosecond laser pulses…

Morphological investigation at the front and rear surfaces of fused silica processed with femtosecond laser pulses in air

Zhaoxin Wu, Hongbing Jiang, Zhaohui Zhang, Quan Sun, Hong Yang, and Qihuang Gong

Department of Physics and State Key Laboratory for Mesoscopic Physics,
Peking University, Beijing 100871, China
hbjiang@mail.phy.pku.edu.cn

http://www.pku.edu.cn

Abstract: Different responses for the front (entrance) and the rear (exit) surfaces of fused silica processed with femtosecond laser pulses at 807 nm were observed under tight focusing conditions (NA = 0.4). The morphology of the surface in the beam path is highly sensitive to the focus position. By adjusting the focus position, we can produce not only a submicrometer cavity but also a submicrometer bubble. We achieved higher-quality micromachining and a better spatial resolution (400 nm) by focusing the laser beam at the rear surface rather than at the front surface.

References and links

1. C. B. Schaffer, A. Brodeur, J. F. Garcia, and E. Mazur "Micromachining bulk glass by use of femtosecond laser pulses with nanojoule energy," Opt. Lett. **26**, 93-95 (2001).
2. Y. Li, K. Itoh, W. Watanabe, K. Yamada, D. Kuroda, J. Nishii, and Y. Jiang, "Three-dimensional hole drilling of silica glass from the rear surface with femtosecond laser pulses," Opt. Lett. **26**, 1912-1914 (2001).
3. J. Krüger and W. Kautek, "The femtosecond pulse laser: a new tool for micromaching," Laser Phys. **9,** 30-40 (1999).
4. L. Shah, J. Tawney, M. Richardson, and K. Richardson, "Femtosecond laser deep hole drilling of silicate glasses in air," Appl. Surf. Sci. **183**, 151-164 (2001).
5. A. Salleo, T. Sands, and F. Y. Génin, "Machining of transparent materials using an IR and UV nanosecond pulsed laser," Appl. Phys. A **71**, 601-608 (2000).
6. P. P. Pronko, S. K. Dutta, J. Squier, J. V. Rudd, D. Du, and G. Mourou, "Machining of sub-micron holes using a femtosecond laser at 800nm," Opt. Commn. **114**, 106-110 (1995).
7. P. Simon and J. Ihlemann, "Ablation of submicron structures on metals and semiconductors by femtosecond UV-laser pulses," Appl. Surf. Sci. **109/110**, 25-29 (1997).
8. E. E. B. Campbell, D. Ashkenasi, and A. Rosenfeld, "Ultra-short-pulse Laser irradiation and ablation of dielectrics," Mater. Sci. Forum **301**, 123-144 (1999).
9. D. Ashkenasi, M. Lorenz, R. Stoian, and A. Rosenfeld, "Surface damage threshold and structuring of dielectrics using femtosecond laser pulses: the role of incubation," Appl. Surf. Sci. **150**, 101-106 (1999).
10. D. Ashkenasi, H. Varel, A. Rosenfeld, S. Henz, J. Herrmann, and E. E. B. Campbell, "Application of self-focusing of ps laser pulses for three-dimensional microstructuring of transparent materials," Appl. Phys. Lett. **72**, 1442-1444 (1998).
11. D. Ashkenasi, A. Rosenfeld, H. Varel, M. Wahmer, and E. E. B. Campbell, "Laser processing of sapphire with picosecond and sub-picosecond pulses," Appl. Surf. Sci. **120**, 65-80 (1997).
12. R. Stoian, M. Boyle, A. Thoss, A. Rosenfeld, G. Korn, I. V. Hertel, and E. E. B. Campbell, "Laser ablation of dielectrics with temporally shaped femtosecond pulses," Appl. Phys. Lett. **80**, 353-355 (2002).
13. E. N. Glezer and E. Mazur, "Ultrafast-laser driven micro-explosions in transparent materials," Appl. Phys. Lett. **71**, 882-884 (1997).
14. D. Wang, C. Li, L. Luo, H. Yang, and Q. Gong, "Sub-diffraction-limit voids in bulk quartz induced by femtosecond laser pulses," Chin. Phys. Lett. **18**, 65 (2001).

15. S. S. Mao, X. L. Mao, R. Greif, and R. E. Russo, "Initiation of an early-stage plasma during picosecond laser ablation," Appl. Phys. Lett. **77**, 2464-2466 (2000).
16. S. S. Mao, X. L. Mao, R. Greif, and R. E. Russo, "Simulation of a picosecond lasr ablation plasma," Appl. Phys. Lett. **76**, 3370-3372 (2000).
17. S. S. Mao, X. L. Mao, R. Greif, and R. E. Russo, "Simulation of infrared picosecond laser-induced electron emission from semiconductors," Appl. Surf. Sci. **127-129**, 206-211 (2000).
18. M. Lenzner, J. Kruger, S. Sartania, Z. Chang, Ch. Spielmann, G. Mourou, W. Kautek, and F. Frausz, "Femtosecond optical breakdown in dielectrics," Phys. Rev. Lett. **18**, 4076-4079 (1998).
19. A. Salleo, F. Y. Génin, M. D. Feit, A. M. Rubenchik, T. Sands, S. S. Mao, and R. E. Russo, "Energy deposition at front and rear surfaces during picosecond laser interation with fused silica," Appl. Phys. Lett. **78**, 2840-2842 (2001).
20. R. Kelly, A. Miotello, B. Braren, and C. E. Otis, "On the debris phenomenon with laser-sputtered polymers," Appl. Phys. Lett. **60**, 2980-2982 (1992).
21. C. B. Schaffer, "Interaction of femtosecond laser pulses with transparent materials," Ph.D. dissertation (Harvard University, Cambridge, Mass., 2001).
22. Z. Wu, H. Jiang, L. Luo, H. Guo, H. Yang, and Q. Gong, "Multiple foci and a long filament observed with focused femtosecond pulse propagation in fused silica," Opt. Lett. **27**, 448- 450 (2002).

1. Introduction

The ultrashort pulse laser is becoming a powerful tool for micromachining and micro-fabrication [1-14]. Compared with nanosecond lasers, femtosecond lasers possess a number of advantages. The shorter time scale for energy coupling into the material reduces the destructive thermal effect, which further leads to higher spatial resolution in surface ablation of metals and semiconductors [6,7]. When a femtosecond laser pulse is focused on a large-bandgap transparent material, the intensity in the focal volume becomes high enough to cause nonlinear absorption such as multiple photon absorption (MPA). MPA leads to a much smaller absorption volume than that of single photon absorption, and it results in a much higher spatial resolution [8,9]. In previous literature [8,9,11] the modifications on the surface of transparent media have been studied in detail. Experiments were conducted in vacuum, and the ultrashort laser pulses were focused at the front (entrance) surface under loose focusing conditions. The modifications in the bulk of transparent materials under tight focusing conditions have also been studied [13,14]. But the laser damage in the bulk of transparent materials is different from the laser ablation on the surface of the materials in ambient gas, which is the interaction among laser field, transparent material, and gas [15-17]. Under tight focusing conditions, the higher resolution of ablation on the surface of a transparent medium may be achieved because of the smaller size of the focal region. However, to our knowledge this probability has not been studied systematically.

In this paper we investigate the ablation effect by focusing the laser beam at the front and rear (exit) surfaces of fused silica in air under tight focusing conditions. In contrast to ablation under loose focusing conditions, the modification on the surface is highly sensitive to the focus position because of the short Rayleigh length. Moreover, by adjusting the distance of the focus to the surface, we can fabricate not only a microcavity but also a microbubble on the surface. By focusing the laser beam at the rear surface rather than at the front surface, we found that the morphology of the destructive area is improved significantly. A submicrometer (400-nm) spatial resolution has been achieved at the rear surface.

2. Experimental setup

In the experiment a Ti:sapphire chirped-pulse amplification laser with a pulse duration of 12 fs, a repetition rate of 10 Hz, and a wavelength of 807 nm was used. Figure 1 shows the schematic of the experimental setup. A spatial filter was employed to obtain a high-quality beam. The objective lens A (Olympus, LCPlan, 20×, 6.9-mm working distance) with a numerical aperture (NA) of 0.40 was used to focus the laser beam. The energy of the input laser pulse was monitored by a calibrated photodiode and adjusted by a half-wavelength plate and a polarizer. A single pulse for each ablation event was chosen by a shutter. All the surfaces of the fused-silica sample were polished, and the thickness of the sample was 3 mm.

The objective lens B (20×, NA = 0.4) and a CCD camera were used to monitor the focus position by capturing the image of the plasma induced in the medium. The pulse duration was measured to be 300 fs at the focal region of objective lens A.
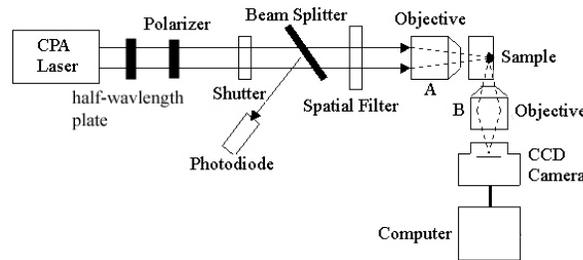

Fig. 1. Experimental setup. CPA, chirped-pulse amplifier.

3. Results and discussion

The morphology of the destructive area on the surface of the sample was measured by atomic force microscopy (AFM; DI, MultiMode scanning probe microscope). The front surface is defined as $z = 0$, and the rear surface is $z = -3$ mm. Figures 2(a)-2(f) show the AFM pictures of laser-induced front surface modifications by means of focusing the laser beam at $z = -4$, -3, 0, 2, and 4 µm with a laser pulse energy of 0.40 µJ.

The morphology of the destructive area on the surface was affected by the focal position of the laser beam. When the energy of a laser pulse is above the breakdown threshold and when the laser is focused into the bulk of a transparent material, it leads to a microexplosion. The laser pulse creates a high-density hot electron plasma with a high temperature and an immensely high pressure. This microexplosion forces the material from the center of the focus outward. A void is thus formed with a densified surrounding [13,14]. As the focus is moved toward the surface, a bubble is formed on the surface, as shown in Fig. 2(a). When the focus is moved further to the surface, the bubble bursts under high pressure, and a pit is formed, as shown in Fig. 2(b). When the focus is located right at the surface, a cavity is formed at the surface, as shown in Fig. 2(c). Moving the focus upstream continuously, we observed that the cavity becomes shallower and eventually disappears. These results are shown in Figs. 2(d) and 2(e). There is no damaged area at the front surface when the focus position is at $z > 4$ µm. In our experiment the diameter of the laser beam at the focus was measured to be 1.9 µm; the Rayleigh length was calculated to be 5.6 µm. This short Rayleigh length leads to the sensitivity of the morphology to the focus position.

Figure 3 shows the AFM pictures of the destructive area at the rear surface of the sample induced by a femtosecond laser pulse with an energy of 0.40 µJ. Figure 3(a) shows the cavity produced by focusing of the laser beam at the rear surface. As the focus of the laser beam is moved into the sample 4 µm from the rear surface, a bubble is formed as shown in Fig. 3(b).

Figures 2(c) and 3(a) show the morphology of the cavities produced when the laser pulse is focused on the front and the rear surfaces of the sample with same pulse energy of 0.40 µJ. Ablation at the rear surface is of a higher quality than at the front surface. In the latter case, the cavity is always surrounded by a ring-shaped protrusion, and there are many sputtered particles on the surface around the cavity, as shown in Figs. 2(b)-2(d). In Fig. 3(a) the produced cavity has a well-defined structure with no debris formed around the cavity, and the polished surface around the damaged area is kept intact. The fringe of the cavity at the rear surface in Fig. 3(a) is also smoother than that at the front surface in Fig. 2(c).

The difference in morphology of the damaged area at the front surface and at the rear surface can be qualitatively explained by the deposition of energy inside the material at the rear surface and plasma backpressure at the front surface. Laser ablation of a solid material consists of several stages, including the formation of a plasma by electronic excitation inside the medium, energy transfer from the plasma to the lattice, medium melting and vaporization
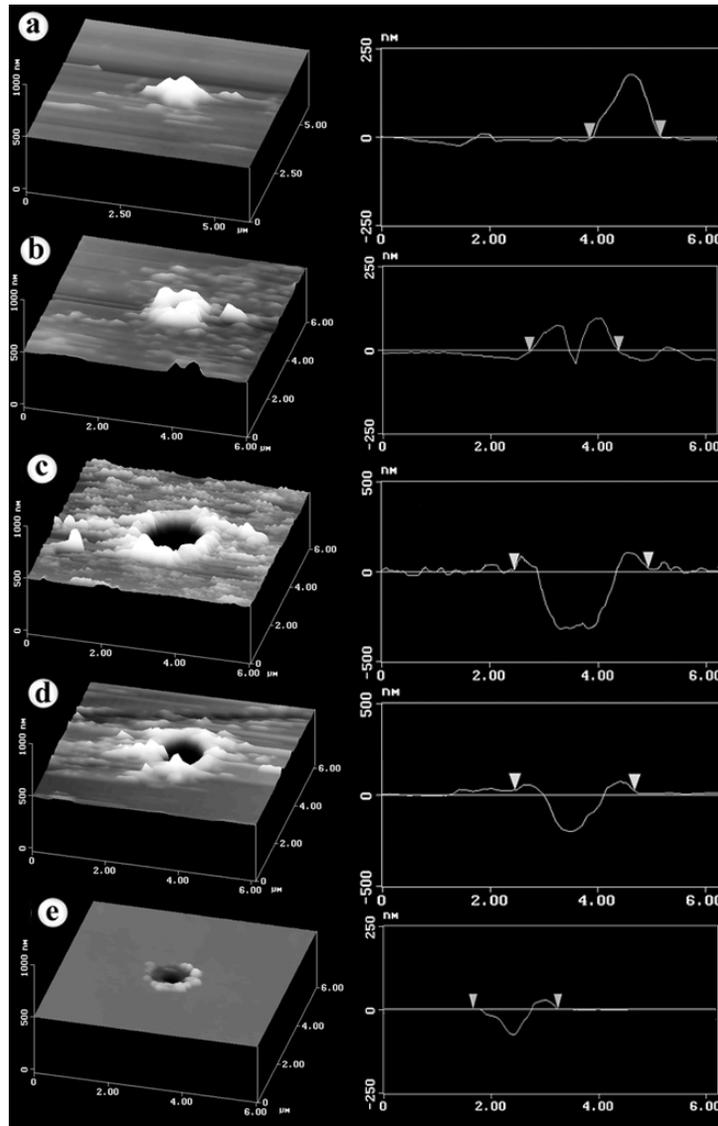
Fig. 2. AFM pictures of the destructive area produced at the front surface. The distance from focus of the laser beam to the front surface is (a) −4, (b) −3, (c) 0, (d) 2, and (e) 4 μm. The negative value represents that the focus is in the bulk side of the sample. The diameter of the damaged area is (a) 1.31, (b) 1.66, (c) 2.48, (d) 2.22, (e) and 1.59 μm. The energy of the laser pulse is 0.40 μm.

followed by the formation of a material vapor plume, and the formation of a shock wave by the interaction between the expanding plume and the surrounding matter. Plasma formation in the bulk medium is a result of multiphoton ionization and avalanche ionization [18]. Ablation in the air with an ultrashort laser pulse, however, also includes avalanche ionization of the air close to the surface. The initial seed electrons for avalanche ionization of the air are provided by electron emission from the surface [15-17]. The directions of electron emission from the front and the rear surfaces with respect to laser beam are opposite, which leads to different

conditions at the two surfaces. On the rear surface the energy of the incident laser pulse is mostly confined inside the material with little avalanche ionization of the air.
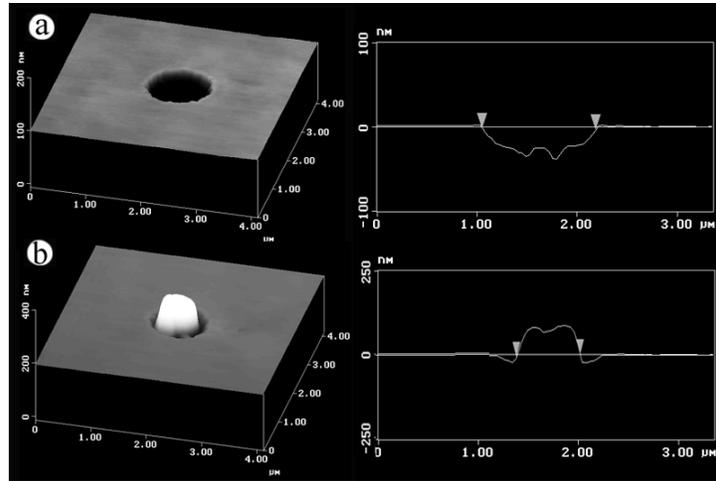

Fig. 3. AFM pictures of the destructive area produced at the rear surface. The laser beam is focused at the rear surface in (a), and in the sample with a distance of 4 µm to the rear surface in (b). The diameter of the cavity is 1.14 µm, and the bubble is 620 nm. The energy of the laser pulse is 0.40 µJ.

In contrast, the interaction between the laser pulse and the plasma inside the bulk causes a large dissipation by air ionization close to the front surface [19]. As a result, the material at the rear surface is more easily ejected, because it is not capped by the plasma backpressure, whereas at the front surface the ejected material can be impeded by the plasma from air ionization, which may lead to the formation of debris around the destructive area [20]. A quantitative interpretation of the difference in morphology of the destructive area by means of focusing the laser beam at the front and the rear surfaces is complicated and is not discussed here. Although the mechanism for laser ablation under ultrashort pulses is complicated, it is clear that the quality of ablation by focusing the laser beam at the rear surface is dramatically improved in comparison with the ablation at the front surface of a transparent medium.

Figure 4 shows the dependences of damaged size at the front and the rear surfaces of the sample on the energy of the laser pulse. The size of the cavity at the rear surface is always smaller than that at the front surface under the same laser energy. For a laser energy of 0.20 µJ, the diameter of the cavity at the rear surface is only 400 nm, as shown in Fig 5. This is the smallest cavity on the rear surface obtained without damaging the bulk of the sample.

The small damaged area and the submicrometer (400-nm) cavity formed at the rear surface were mainly attributed to the combined effect of self-focusing and multiple photon absorption. In contrast to the damage at the front surface, self-focusing plays an important role in laser ablation at the rear surface. It can lead to smaller sized cavities. The effect of self-focusing by various NA objectives in fused silica has been studied in detail by Mazur's group [1,13,21], and in our previous study on filamentation of a focused laser pulse in fused silica [22]. It was found that for a 0.40-NA objective lens, the self-focusing effect would significantly reduce the beam waist in fused silica.
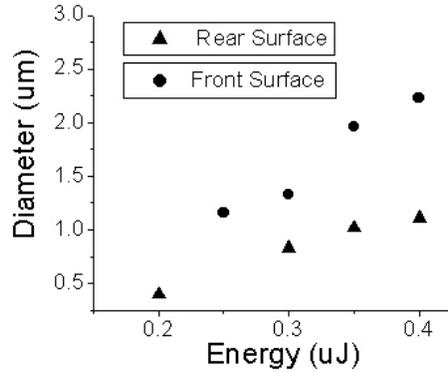
Fig. 4. Plotted is the dependence of diameter of damaged area at the front and rear surface of sample on the energy of the single laser pulse. The laser beam was focused by the objective with 0.40-NA and 6.9-mm working distance.
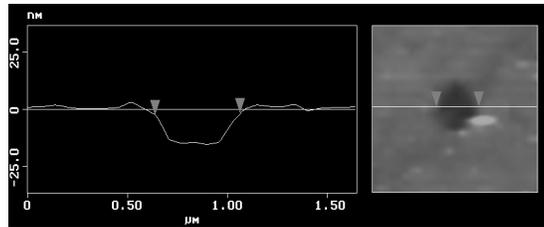

Fig. 5. AFM image of the pit produced by means of focusing the laser pulse at the rear surface of the sample. The diameter of the pit is 400 nm, and the laser pulse energy was 0.20 µJ.

4. Conclusion

Femtosecond laser ablation at the front and rear surfaces of fused silica was investigated under tight focusing conditions. The morphology of the destructive area on the surface was observed to be sensitive to the distance for the focus position to the surface. This is a result of the short Rayleigh length of the laser beam under tight focusing conditions. On the surface of the sample, we could fabricate not only a cavity but also a bubble by adjusting the relative position of the focus with respect to the surface. The morphology of the destructive area under ablation at the rear surface exhibits a higher quality than at the front surface. The cavity at the rear surface is well defined and without debris. Moreover, a submicrometer (400-nm) spatial resolution for surface micromachining is achieved at the rear surface because of self-focusing. These results demonstrate a powerful tool for micromachining with well-defined and clean structures and submicrometer resolution in transparent media.